REPORT DOCUMENTATION PAGE

Form Approved
OMB No. 0704-0188

1. REPORT DATE *(DD-MM-YYYY)*	2. REPORT TYPE	3. DATES COVERED *(From - To)*
02-07-2008	Technical Paper	

4. TITLE AND SUBTITLE

Effect of Chamber Wall Proximity on Radiometer Force Production (Preprint)

5a. CONTRACT NUMBER

5b. GRANT NUMBER

5c. PROGRAM ELEMENT NUMBER

6. AUTHOR(S)
N.P. Selden (USC); N.E. Gimelshein, S.F. Gimelshein (ERC); A.D. Ketsdever (AFRL/RZSA)

5d. PROJECT NUMBER

5e. TASK NUMBER

5f. WORK UNIT NUMBER
50260542

7. PERFORMING ORGANIZATION NAME(S) AND ADDRESS(ES)

Air Force Research Laboratory (AFMC)
AFRL/RZSA
10 E. Saturn Blvd.
Edwards AFB CA 93524-7680

8. PERFORMING ORGANIZATION REPORT NUMBER

AFRL-RZ-ED-TP-2008-288

9. SPONSORING / MONITORING AGENCY NAME(S) AND ADDRESS(ES)

Air Force Research Laboratory (AFMC)
AFRL/RZS
5 Pollux Drive
Edwards AFB CA 93524-7048

10. SPONSOR/MONITOR'S ACRONYM(S)

11. SPONSOR/MONITOR'S NUMBER(S)
AFRL-RZ-ED-TP-2008-288

12. DISTRIBUTION / AVAILABILITY STATEMENT

Approved for public release; distribution unlimited (PA #08284A).

13. SUPPLEMENTARY NOTES
For presentation at the 26th International Symposium on Rarefied Gas Dynamics, Kyoto, Japan, 21-25 July 2008.

14. ABSTRACT

The impact of chamber wall location on a radiometric device has been studied experimentally and numerically in chambers from 0.2m to 1.8m in diameter with background pressure ranging from 0.006 to 1Pa. The range of pressures investigated is broad enough to observe the impact of the chamber walls on a given radiometer configuration in both the free molecule and transitional regimes. The contribution of the chamber walls to both the flowfield structure and radiometric force production were examined for helium, argon, and nitrogen test gases. Various radiometer geometries were experimentally tested on a force balance, with nano-Newton resolution, placed in a stagnant gas. The computational results were obtained using the solution of the model kinetic equations and by the direct simulation Monte Carlo method. The simulations compliment the experimental work by varying the chamber dimensions to a degree not practically attainable, demonstrating both the decreasing temperature gradient of the flowfield and the reduced force production of the radiometer as the physical dimensions of the chamber increase. It is concluded that chamber wall location has a dramatic effect on the force production of a radiometer, especially at higher pressures, where increasing the distance from the vane to the wall reduces both temperature gradient and the total force produced.

15. SUBJECT TERMS

16. SECURITY CLASSIFICATION OF:			17. LIMITATION OF ABSTRACT	18. NUMBER OF PAGES	19a. NAME OF RESPONSIBLE PERSON
					Dr. Andrew Ketsdever
a. REPORT	b. ABSTRACT	c. THIS PAGE	SAR	8	19b. TELEPHONE NUMBER *(include area code)*
Unclassified	**Unclassified**	**Unclassified**			N/A

Standard Form 298 (Rev. 8-98)
Prescribed by ANSI Std. 239.18

Effect of Chamber Wall Proximity on Radiometer Force Production (Preprint)

N.P. Selden[a], N.E. Gimelshein[b], S.F. Gimelshein[b], and A.D. Ketsdever[c]

[a]*University of Southern California, Los Angeles, CA 90089*
[b]*ERC Incorporated, Huntsville, AL 35805*
[c]*Air Force Research Laboratory, Edwards AFB, CA 93524*

Abstract. The impact of chamber wall location on a radiometric device has been studied experimentally and numerically in chambers from 0.2m to 1.8m in diameter with background pressure ranging from 0.006 to 1Pa. The range of pressures investigated is broad enough to observe the impact of the chamber walls on a given radiometer configuration in both the free molecule and transitional regimes. The contribution of the chamber walls to both the flowfield structure and radiometric force production were examined for helium, argon, and nitrogen test gases. Various radiometer geometries were experimentally tested on a force balance, with nano-Newton resolution, placed in a stagnant gas. The computational results were obtained using the solution of the model kinetic equations and by the direct simulation Monte Carlo method. The simulations compliment the experimental work by varying the chamber dimensions to a degree not practically attainable, demonstrating both the decreasing temperature gradient of the flowfield and the reduced force production of the radiometer as the physical dimensions of the chamber increase. It is concluded that chamber wall location has a dramatic effect on the force production of a radiometer, especially at higher pressures, where increasing the distance from the vane to the wall reduces both temperature gradient and the total force produced.

Keywords: Radiometric force, experimental and numerical modeling, chamber wall effect.
PACS: 51.10.+yhttp://www.aip.org/pacs/index.html

INTRODUCTION

The existence of forces created in rarefied environments by temperature gradients is now well known, but a deep understanding of the mechanics of their formation and interaction with nearby surfaces is far from complete. The foundation for the existence of these forces was laid by Fresnel[1] who, in 1825, observed a repulsion of two thin foil veins in an evacuated container. It was not until nearly half a century later that William Crookes[2] invented what is now known as a radiometer, which allowed a number of prominent scientists of the time to test a variety of theories[3] about the sources of these forces. While the bulk of the work in this period focused on the interaction of the gas molecules with the radiometer vane, comparatively little work was done on the interaction of the entire system with the walls of the vacuum vessel. Despite the fact that Schuster[4] had shown as early as 1876 that the container was also affected by the moving gas, another 40 years passed before any focused experimental work was done in this regard.

As with many important advances in science, West[1] stumbled onto his contribution in 1919 while exploring an entirely different topic. Seeking to measure the pressure of light, he found (as had several others before him) that his measurements were disturbed due to the presence of a temperature gradient in his experiment. Noting that the disturbances grew in size as his piece of foil was moved further from the centerline of an evacuated tube, he proceeded with a series of experiments designed to explore interaction with the container. He surmised that while radiometric forces should be miniscule in his apparatus, the asymmetry of the experiment itself created non-equilibrium conditions in the gas. Ultimately he concluded with three main ideas: at the lowest background pressures the force on the foil varied with the square root of gas temperature; thermal transpiration was the cause of the disturbances at higher pressures; and finally the gas gradient along the face was significantly more important than the surface gradient along the edge. As a point of reference, West demonstrated, that at higher pressures, halving the distance to the vessel wall doubled the force on the foil strip.

An even more exhaustive study was undertaken by Brüche and Littwin[5] in the late 1920's. In their comprehensive work they covered an extremely large experimental matrix including a variety of gases, radiometer geometries, and separation distances. One of the main conclusions of their work was a formula for the relationship between force and pressure showing an almost Gaussian response to the natural log of pressure. A second conclusion, and one of great relevance to the understanding of the impact of the chamber wall, was verification of West's conclusion that at high pressures the force on the vane scales with the inverse of the distance.

It is useful to explore why this is so. Under collisionless conditions, the radiometer has an extremely large force production potential. It has been shown[1,2] that an increase in pressure will result in a proportional increase in the force. If maintaining these conditions were possible and the linear increase were allowed to continue, a radiometer of area $1m^2$ at an atmosphere pressure and a temperature difference of 10K would produce forces of approximately 700N. In reality, the onset and dominance of collisions at higher pressures causes the force production to rapidly decline. This force decay can be slowed by moving the vane location closer to the chamber wall. In this manner, every halving of the distance to the chamber wall also halves the number of intermolecular collisions of the average molecule as it traverses the space between the device and vessel. Taken to the limit of a mean-free path of separation, every molecule impinging on the vane would in effect behave as if it were collisionless with respect to other gas molecules.

The observations and conclusions of the past gained their importance recently with the advent of Microelectromechanical Systems (MEMS) type fabrication, as well as the ongoing search for viable near-space propulsion technologies. Over the last decade, researchers have started to reconsider radiometer-type devices and their possible applications in both the micro- and the macro-scale. Examples of these applications include novel micro-actuators[6], laser opto-engines[7], and high altitude lifting devices[8]. To optimize their performance, it is important to understand the impact of the chamber on the flowfield. In the first two applications noted above, the chamber plays a dominant role, and in the final application, the complete lack of a chamber has a significant negative impact on the total force produced. The focus of this work is to explore the "chamber effect" in an attempt to better understand the limiting cases of both extremely large and extremely small chambers. Both experimental and computational approaches are undertaken, and the comparison of the two methods is used to explore the radiometric forces produced.

EXPERIMENTAL SETUP

To study the effects of the chamber on the production of radiometric forces on a plate, a circular vane device was used. The device consisted of a Teflon insulator placed between two aluminum plates, each plate having a thickness of 0.318cm. A resistive heater was affixed between one of the aluminum plates and the Teflon insulator, and the entire device was assembled using eight low-thermal conductivity nylon machine screws with 2.13mm diameters. The assembled device has a total device thickness of 0.95cm, with a diameter of 11.13cm and is shown in Fig. 1. When coupled with a DC power supply the resistive heater was used to maintain a consistent power input of approximately 8W to the radiometer vane, and the entire device was allowed to come to thermal equilibrium under vacuum.

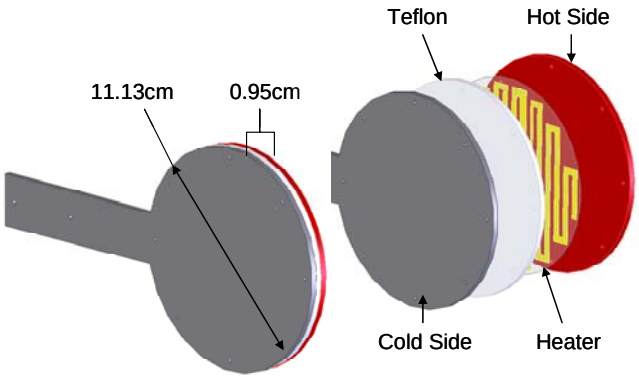

FIGURE 1. CAD drawing of radiometric device

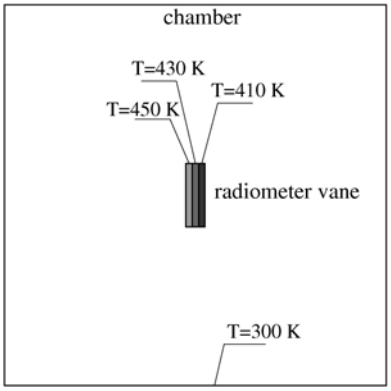

FIGURE 2. Computational domain

The radiometer was mounted on a modified version of the nano-Newton Thrust Stand (nNTS)[9] located inside either the 0.4m or 3.0m diameter vacuum chamber. When calibrated using a set of electrostatic combs[10], the nNTS provides very accurate and repeatable data with typical force resolution of approximately 0.1μN and statistical scatter around 1%. For the current experiment, the experimental error based on standard deviation ranges from a few percent at the lowest pressures to less than 1% through most of the curve. However, due to the normalization by experimental temperature measurements, variation of the background pressure, and the small uncertainty of the calibration method, the total absolute experimental uncertainty is ~4%. Daily variations of multiple data sets have been observed to be ~2%.

The experimental data was obtained by evacuating the chamber to a base pressure below 10^{-3} Pa. A constant voltage was applied to the heater, and this resulted in the main surfaces reaching temperatures of approximately 415K (hot) and 365K (cold). The background pressure inside the chamber was varied by flooding the chamber with argon, helium, and nitrogen over a range of pressures from 0.1Pa to 1.0Pa.

The experimentally measured force was normalized by the temperature difference between the hot and cold plates, ΔT, for the purpose of comparing results for different pressures and chambers. Verification of the validity of the experimental normalization method is demonstrated in a previous paper[11], where exceptional linearity with temperature difference is observed.

COMPUTATIONAL SETUP

Two kinetic numerical approaches are used in this work. The first is the direct simulation Monte Carlo (DSMC) method, the most widely used method of rarefied gas dynamics. While a DSMC solution represents a statistical solution to the master kinetic equation, the method becomes very expensive, and often impractical, when subtle details of low speed flows need to be examined. The second approach is the deterministic solution of the ellipsoidal statistical (ES) model kinetic equation, which lacks the accurate representation of the collision term, but has benefit of the absence of statistical fluctuations inherent in DSMC.

The DSMC computational tool, SMILE[12], was used in all DSMC computations presented in this work. The variable hard sphere model with parameters[13] was used for the intermolecular potential, and the Larsen-Borgnakke model with variable rotational relaxation number used for the translational-internal energy transfer. The gas-surface model was assumed to be diffuse with full energy and momentum accommodation. A two-dimensional module of SMILE was used in this work because three-dimensional modeling is prohibitively expensive for most pressures under consideration. The schematic of the numerical setup is shown in Fig. 2. The computations were conducted for two plates with dimensions 0.95x3.81cm and 0.95x7.62cm immersed in an initially uniform stagnant gas in a chamber. The third (Z axis) dimension of 12.7cm was assumed when calculating forces consistent with the actual size of the plate in the previous experimental study. The main surfaces of the plate were set to 410K (cold) and 450K (hot), and the intermediate sidewalls were 430K. The chamber wall temperature was assumed to be constant at 300K. The computations were performed for different chamber pressures and chamber sizes from 0.45cm to 1.8m using two gases, helium and argon. The number of simulated molecules varied from 2 to 10 million and the number of cells varied from 0.5 to 5 million depending on the chamber size and gas pressure, always satisfying the standard DSMC requirements.

A finite volume solver SMOKE developed at ERC, Inc. has been used to deterministically solve the ES model kinetic equation. SMOKE is a parallel code based on conservative numerical schemes developed by L. Mieussens[14]. A second order spatial discretization is used along with implicit time integration. Fully diffuse reflection with complete energy accommodation is applied at the vane and chamber walls. A symmetry plane (symmetry axis in axisymmetric computations) was set at the lower boundary. The grid convergence was achieved by increasing the number of spatial nodes and points in the velocity space. The latter one was (18,18,12) for the results presented below, and the number of cells varied from 5,000 to 50,000 depending on the chamber size.

RESULTS

The impact of the chamber walls has been studied using the DSMC method for a helium flow at 2Pa, where the radiometric force is near its maximum, with the chamber size varying from below 0.2m to about 1.8m with the boundary conditions on the plate and chamber walls unchanged. The analysis of the flowfield shows that when the chamber is about a hundred times larger than the heated plate, there is still a pronounced effect of the location of the chamber walls on the flow properties not only near the chamber walls, but also near the plate. This is illustrated in

Fig. 3 where the temperature profiles are shown for different chamber sizes in the cross section perpendicular to the vane and coming through its center. The plate center is at X=0.

Generally, the increase in the chamber size results in a decrease of temperature and pressure gradients near the plate. As a result, the net force exerted on the vane decreases for larger chamber sizes, as shown in Fig. 4. It is also shown that a rapid increase in force occurs as the chamber size decreases, and it is expected to further increase until the free molecular limit is reached. Note also that full convergence has not been obtained even as the chamber size was over 40 times larger than the vane. Larger chamber sizes were not considered due to prohibitively high computational cost (the run for the 1.8m chamber case took over a week on a 40 processor cluster).

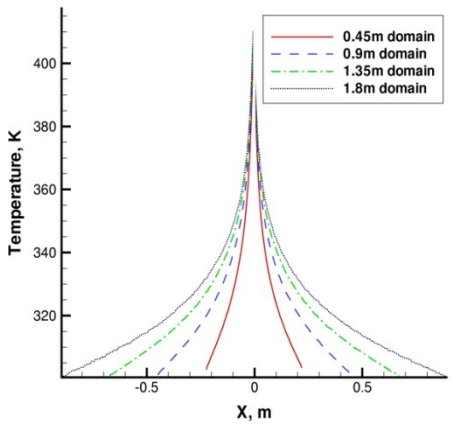

FIGURE 3. Temperature gradient in helium as a function of chamber dimension

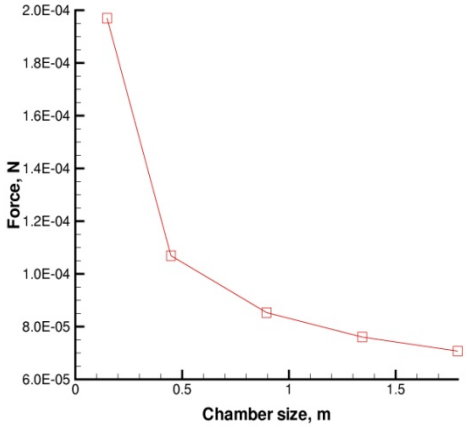

FIGURE 4. Force as a function of chamber size

The impact of statistical scatter for the other two gases under consideration, nitrogen and argon, was even higher than for helium. Next, the study of the influence of the chamber size was conducted using the solution of ES model equation. The macroparameters obtained with the model equation were found to be close to those calculated with DSMC, as shown in Fig. 5. In this figure, the gas temperature field and the streamlines are presented for argon at a pressure of 1.2 Pa, with the ES solution plotted at the top and the DSMC, at the bottom. The difference between these results is less than or about 1K. The streamlines in both solutions show two counterpropagating vortices: a large clockwise vortex formed in front of the hot side of the vane, and a much smaller counterclockwise vortex observed near the cold side. This is different from the conventional cold-to-hot flow structure. The ES computations showed that the transition from the four vortex structure to a more conventional two-vortex structure, with two large vortices transferring gas from cold to hot side of the vane, occurs at higher gas pressures. This is illustrated in Fig. 6 where the vortex structure in argon is shown for 0.6 Pa at the bottom and 6 Pa at the top.

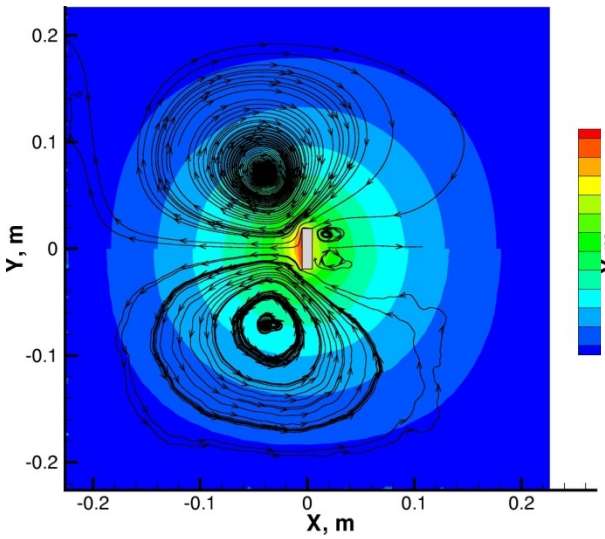

FIGURE 5. ES (top) and DSMC (bottom). Argon, 1.2Pa

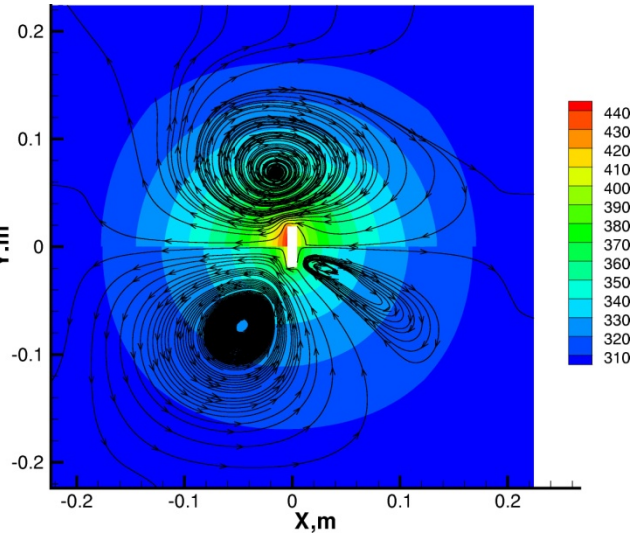

FIGURE 6. Vortex structure: 0.6 Pa (bottom) and 6 Pa (top).

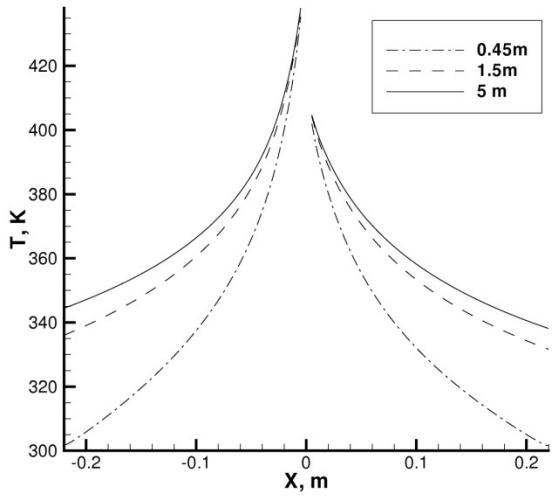

FIGURE 7. Temperature gradients in argon for different chamber sizes

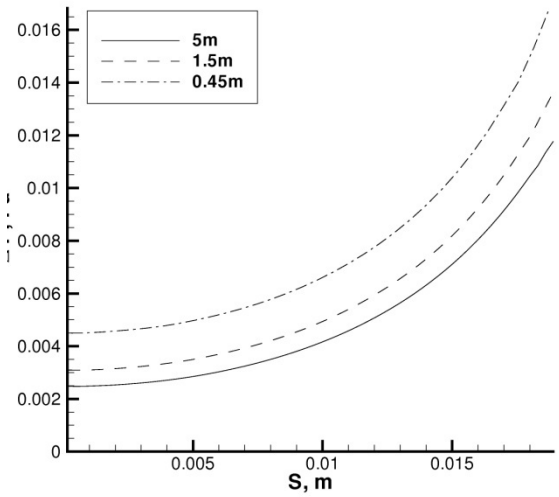

FIGURE 8. Resulting pressure on the plate

The influence of the chamber size on the gas temperature distribution near the plate, obtained through the solution of the model equation for a pressure of 3Pa in argon, is shown in Fig. 7 in the cross section perpendicular to the vane and coming through its center. Note that only a part of the domain is shown here. It is clear that even in the vicinity of the vane, the gas is impacted by the location of the chamber walls; the closer the chamber wall with a relatively low temperature of 300K, the colder the gas near the vane. For the larger chamber sizes, the gas molecules reflected on the chamber walls have more time to adjust to the vane temperature as they approach the vane, which results in lower total force. The change in the distributed force depends on the location on the plate. This is illustrated in Fig. 8, where the difference between the pressure on the hot and cold sides of the vane is shown versus distance along the plate. Here, S=0 corresponds to the center of the vane. Generally, the resulting distributed pressure difference is larger toward the edge of the plate. The increase in the chamber size from 0.45m to 1.5m causes an increase in pressure of about 0.003Pa near the center and over 0.04Pa closer to the edge.

The computed results for argon at different pressures are given in Table 1, where the normal force in N/m is shown for four different chamber sizes. For all pressures, the convergence of the total force versus the chamber size was not obtained for the 5m chamber.

TABLE 1. Force production in various chambers

Pressure, Pa	0.45m	1.5m	3m	5m
0.122	5.21E-006	4.64E-006	4.29E-006	4.12E-006
0.300	1.07E-004	7.81E-005	6.96E-005	6.62E-005
0.600	1.32E-004	1.00E-004	8.83E-005	8.41E-005
1.200	1.49E-004	1.12E-004	1.00E-004	9.28E-005
2.000	1.48E-004	1.14E-004	1.02E-004	9.60E-005
3.000	1.41E-004	1.12E-004	1.01E-004	9.50E-005

All previous numerical results were obtained for a two-dimensional flow. As expected, the chamber size convergence was much faster for axisymmetric flow, where same chamber size as in 2D size corresponds to a much larger chamber wall to vane wall area ratio. For example, for a vane with dimensions similar to that of the experimental setup, the force on the vane decrease only by 2 to 3% for pressures between 0.1 and 0.6Pa. This means that the larger chamber used in the experiments is virtually independent of the chamber wall effects.

Experimental results for nitrogen in the both the large and small chambers are presented in Fig. 9. While similar trends are observed, it is obvious that the chamber itself has a dramatic effect. For the large chamber, the peak of each device occurs at approximately half the pressure of the peak in the small chamber. There is also a noticeable decrease in the maximum force, as the largest measured data in the small chamber was 1.28×10^{-6} N/K while in the large it was 7.53×10^{-7} N/K. As the pressure increases, the force becomes noticeably stronger in the smaller chamber. This makes physical sense when compared with a limiting case of a chamber that is only slightly larger than the device; the vane will behave as if no intermolecular collisions occur if the mean free path of a gas

molecule is longer than the distance between the device and the chamber wall. For each device the data behaves as predicted in the low pressure region, where it can be presumed that vortex and collisional contributions are minimal.

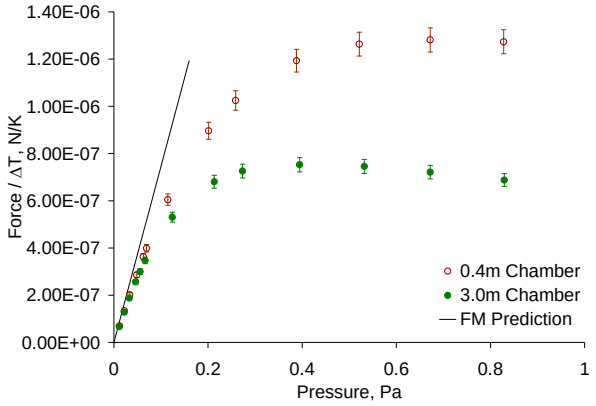

FIGURE 9. Measured experimental force in two chambers

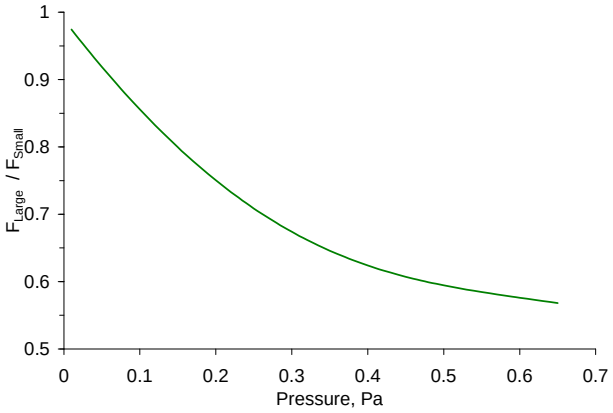

Figure 10. Force ratio showing pressure dependence

Further understanding of the pressure dependence of the chamber effect is gained by taking the ratio of the force produced by the large plate and that produced by the small one. As shown in **Error! Reference source not found.** Fig. 10, the ratio at the lowest pressures trends towards unity, which implies that the chamber walls have very little effect at the lowest pressures. The rapid decrease in the ratio as pressure increases demonstrates the importance of the chamber effect and the increasing force production of the radiometer in the small chamber.

CONCLUSION

A study of the radiometric forces on heated plates has been conducted both experimentally and computationally. The experiments were performed in two vacuum chambers up to a maximum pressure of 1 Pa for various carrier gases. The computations were performed with the DSMC method for a 2-D gas flow over a comparable range of pressures. Qualitatively the experimental data and computational results are similar, demonstrating that the size of the chamber in which the radiometer resides is of primary importance. Especially at higher pressures near the peak force production of the device, the size of the chamber is inversely related to the generated force.

ACKNOWLEDGMENTS

The work at USC was supported in part by the Propulsion Directorate of the Air Force Research Laboratory at Edwards Air Force Base, California. The work at ERC was supported by AFOSR. The authors thank Dr. Ingrid Wysong and Dr. E.P. Muntz for many fruitful discussions.

REFERENCES

[1]A. Fresnel, Annales de Chimie et de Physique, {29}, 57 (1825)
[2]W. Crookes, "On attraction and repulsion resulting from radiation," Phil. Trans. R. Soc., {165} 519 (1875)
[3]G.D. West, "A modified theory of the Crookes radiometer," Proc. Phys. Soc. London, {32} 222 (1919)
[4]A. Schuster, Phil. Trans. R. Soc., {166} 715 (1876)
[5]E. Brüche, W. Littwin, "Experimental contributions to the radiometer question," Z. Physik, {52,} 318 (1928)
[6]D.C. Wadsworth, E.P. Muntz, *J. MEMS*, **5**(1), 59 (1996)
[7]M. Ota, T. Nakao, M. Sakamoto, *Mathematics and Computers in Simulation*, **55**, 223, 2001
[8]G. Benford, J. Benford, *Acta Astronautica*, **56**, 529 (2005)
[9]A.J. Jamison, A.D. Ketsdever, E.P. Muntz, *Review of Scientific Instruments*, **73**, 3629 (2002)

[10]N.P. Selden, A.D. Ketsdever, “Comparison of force balance calibration techniques for the nano-Newton range,” Review of Scientific Instruments, Vol. 74, 5249-5254.
[11]N. Selden, C. Ngalande, S. Gimelshein, and A. Ketsdever, “Experimental and Computational Observation of Radiometric Force on a Plate,” AIAA Thermophysics Conference, June 2007
[12]Ivanov, M.S., Markelov, G.N., Gimelshein, S.F. “Statistical simulation of reactive rarefied flows: numerical approach and applications,” AIAA Paper 98-2669, June 1998.
[13]Bird, G.A., *Molecular Gas Dynamics and the Direct Simulation of Gas Flows*, Clarendon Press, Oxford, 1994.
[14]Mieussens, L., "Discrete-Velocity Models and Numerical Schemes for the Boltzmann-BGK Equation in Plane and Axisymmetric Geometries", *Journal of Computational Physics*, Vol. 162, 2000, pp. 429-466.